


## CASE IMAGE

# A 6-year-old female with synchronous cerebellar and thalamic masses

Wenjun Luo<sup>1,2,3</sup>  | Cuiyun Sun<sup>1,2,3</sup> | Zhendong Jiang<sup>1,2,3</sup> | Rongju Zhang<sup>4</sup> | Wengao Zhang<sup>5</sup> | Shizhu Yu<sup>1,2,3</sup>

<sup>1</sup>Department of Neuropathology, Tianjin Neurological Institute, Tianjin Medical University General Hospital, Tianjin, China

<sup>2</sup>Tianjin Key Laboratory of Injuries, Variations and Regeneration of the Nervous System, Tianjin, China

<sup>3</sup>Key Laboratory of Post-trauma Neuro-repair and Regeneration in Central Nervous System, Ministry of Education, Tianjin, China

<sup>4</sup>Department of Pathology, Cangzhou Central Hospital, Cangzhou, China

<sup>5</sup>Department of Neurosurgery, Cangzhou Central Hospital, Cangzhou, China

## Correspondence

Shizhu Yu, Department of Neuropathology, Tianjin Neurological Institute, Tianjin Medical University General Hospital, No. 154, Anshan Road, Tianjin 300052, China.  
Email: [tjyushizhu@163.com](mailto:tjyushizhu@163.com)

## 1 | CASE PRESENTATION

A 6-year-old girl was admitted to our hospital for sudden-onset headache with vomiting. Ataxia was observed via physical examination, and two well-defined lesions were identified via MRI, one in the left cerebellum, measuring approximately 42 mm × 37 mm in size, which was mainly T1-hyperintense, T2-hypointense (Figure 1), with T1-hypointense and T2-hyperintense in

### BOX 1 Virtual glass slide

Access at <https://isn-slidearchive.org/?col=ISN&fol=Archive&file=BPA-24-04-CI-103-cerebellum.svs> and <https://isn-slidearchive.org/?col=ISN&fol=Archive&file=BPA-24-04-CI-103-thalamus2.svs>.



**FIGURE 1** MRI shows T2-weighted images of the cerebellar lesion and the thalamus lesion (inset).

its inner and edge parts, and without enhancement in the center of T1-weighted postcontrast, and the other in the right thalamus, which was cystic, measuring 15 mm × 15 mm, with T2-hyperintense (Figure 1, inset) and T1-hypointense, both of which provided the first impressions of hemorrhagic lesions. The cerebellar lesion was excised for definitive diagnosis and symptom relief, whereas the thalamic lesion was left under close monitoring and eventually removed 5 months later after another episode of headache due to a volume increase confirmed by MRI in the patient's local hospital (Box 1).

## 2 | FINDINGS

Haematoxylin and eosin (H&E) staining revealed that the cerebellar tumour was predominantly solid with

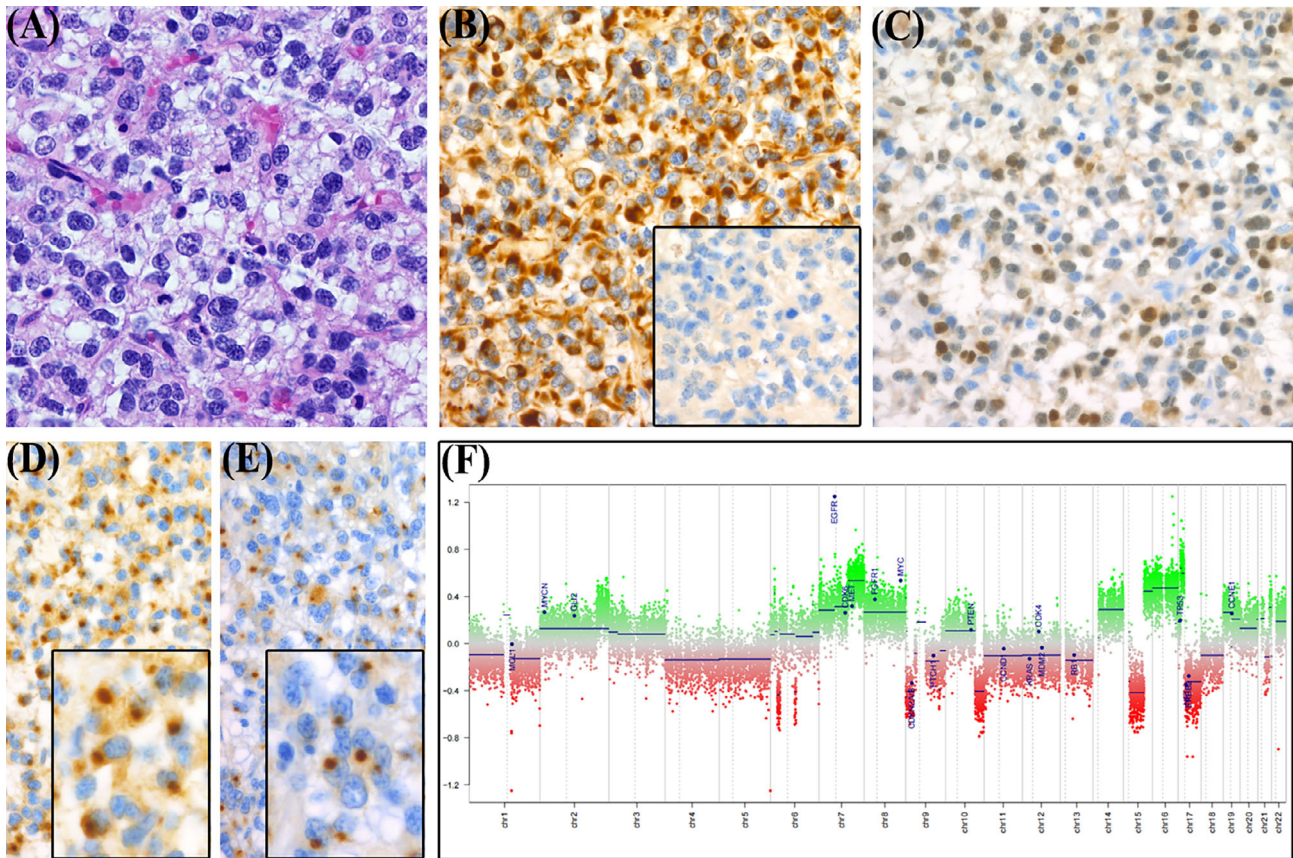


**FIGURE 2** Histological and immunohistochemical features. (A) Oligodendroglial-like cells with branching capillaries and mitoses (40 $\times$ ). GFAP (B), NeuN (C), SYN (D), and EMA (E) are positive, while OLIG2 is negative (B inset) (40 $\times$ ). (F) The CNV profile from DNA methylation analysis shows EGFR amplification and gain of chromosomes 7, 8, 16, 14q and 17 p.

medium cell density. The tumour cells were uniform, mainly with clear vacuolated cytoplasm and elongated processes. Oligodendroglial-like cells were observed in some areas (Figure 2A), and branching capillaries were scattered in the stroma, along with intratumoural hemorrhage and cystic alterations (Box 1). Mitoses were easily observed (5 mitoses per 10 HPF), but microvascular proliferation and palisading necrosis were absent. Immunohistochemical staining revealed that GFAP (Figure 2B), CD56 and H3K27me3 were diffusely positive; S-100 and p53 were mostly positive; and nearly half of the tumour cells were NeuN positive (Figure 2C), whereas OLIG2 was negative (Figure 2B, inset). Synaptophysin (SYN) and EMA immunoreactivities were notably present in a significant portion of the tumour cells in a paranuclear dot-like pattern (Figure 2D,E, inset). The Ki-67 labelling index was 15%.

During whole-exome high-throughput sequencing, two clinically relevant alterations, *EGFR* amplification and *TP53* mutation, were found. The paraffin-embedded tumour tissue was then subjected to a genome-wide DNA methylation assay via the Human Methylation 850K array platform. The methylation profile in version 12.8 of the publicly accessible Heidelberg classifier matched the methylation class 'diffuse paediatric-type high-grade

glioma (pHGG), H3-wild type and IDH-wild type' RTK2 (pHGG RTK2), with a score >0.9. MGMT promoter methylation was present. The copy number profile derived from the methylation array revealed changes consistent with *EGFR* amplification and gains of chromosomes 7, 8, 16, 14q and 17 p.

The thalamic lesion operation was performed at the patient's local hospital. The histopathological and immunohistochemical features of the thalamic lesion were consistent with the cerebellar lesion after careful comparison by two independent pathologists. Unfortunately, extensive bleeding made the thalamic tumour sample unsuitable for independent molecular testing.

### 3 | DIAGNOSIS

Diffuse paediatric-type high-grade glioma, H3-wild type and IDH-wild type, RTK2 subtype, CNS WHO grade 4.

### 4 | DISCUSSION

As a new entity in the 2021 WHO CNS tumours classification, diffuse paediatric-type high-grade glioma,

H3-wild type and IDH-wild type (pHGG) currently comprise three subtypes: pHGG RTK1 (frequently associated with *PDGFRA* amplification), pHGG RTK2 (enriched in *EGFR* amplification and *TERT* promoter mutation) and pHGG MYCN (enriched for *MYCN* and *ID2* amplification) [1, 2]. The diagnosis of pHGG relies heavily on molecular and methylation profiling, while the histological and immunochemical features remain inadequately documented, particularly for subtype RTK2. The main histological features of this case included branching capillaries and cells with clear vacuolated cytoplasm and elongated processes, along with frequent mitoses and a high Ki-67 index. Microvascular proliferation was absent in both cerebellar and thalamic lesions. However, the thalamic lesion showed higher cell density with palisading necrosis, which was different from the cerebellar lesion. The two lesions were completely separated on MRI without any discernible imaging connections. The histopathological similarities indicate this case may represent a multifocal pHGG. The increased cell density and palisading necrosis of the thalamic lesion compared to the cerebellar one may have occurred over time. However, the possibility that these two lesions are molecularly distinct high-grade gliomas cannot be excluded.

Immunohistochemically, pHGG typically expresses at least one glial marker (GFAP and/or OLIG2) or one neuronal marker, with preserved H3K27me3 expression [2]. In our patient, GFAP and H3K27me3 were diffusely positive, while OLIG2 was negative despite oligodendroglioma-like features, consistent with minimal OLIG2 expression in pHGG RTK2 [3]. Neuronal markers NeuN, S-100, SYN and CD56 showed varying positivity, with paranuclear dot-like immunoreactivity for SYN and EMA. Although both of them can be found in oligodendroglioma and ependymoma, respectively, simultaneous expression of SYN and EMA in pHGG has previously been unreported. It will be interesting to observe whether subsequent case reports have these phenotypic features and whether these features are helpful for diagnosis. The major findings in genome-wide methylation sequencing revealed an unmethylated status of the MGMT promoter, characteristic of pHGG RTK2, alongside *EGFR* amplification, *TP53* mutation and chromosome 7 acquisition, also seen in adult glioblastomas [1]. The overlapping morphology and genetics highlight the need for integrated pathological and molecular analyses to differentiate pHGG RTK2 from adult glioblastoma.

In terms of clinical outcomes, our patient did not receive additional treatment after surgical resection and has been followed for 18 months without recurrence.

## KEYWORDS

diffuse paediatric-type high-grade glioma, H3-wild type and IDH-wild type, RTK2

## AUTHOR CONTRIBUTIONS

Wenjun Luo designed the case report and wrote the manuscript. Cuiyun Sun provided and interpreted the histology analysis. Zhendong Jiang stained slices of the tumour tissue. Rongju Zhang analysed the slides of the thalamic tumour. Wengao Zhang provided the slides of the thalamic tumour. Shizhu Yu reviewed the histology analysis and MRI scans. All authors revised and approved the final manuscript and agreed to be accountable for all aspects of the work.

## ACKNOWLEDGEMENTS

The authors want to thank Xiaohong Yao, Institute of Pathology and Southwest Cancer Center, Southwest Hospital, Third Military Medical University (Army Medical University), for her work on genome-wide DNA methylation profiling.

## FUNDING INFORMATION

No external or internal funding or support was required for this case report.

## CONFLICT OF INTEREST STATEMENT

The authors have no conflicts of interest to disclose.

## DATA AVAILABILITY STATEMENT

All data generated or analysed during this study are included in this article. Further enquiries can be directed to the corresponding author.

## ORCID

Wenjun Luo  <https://orcid.org/0000-0003-2811-1848>

## REFERENCES

1. Korshunov A, Schrimpf D, Ryzhova M, Sturm D, Chavez L, Hovestadt V, et al. H3-IDH-wild type pediatric glioblastoma is comprised of molecularly and prognostically distinct subtypes with associated oncogenic drivers. *Acta Neuropathol.* 2017;134(3): 507–16.
2. WHO Classification of Tumours Editorial Board. World Health Organization classification of tumours of the central nervous system. 5th ed. Lyon: International Agency for Research on Cancer; 2021.
3. Aboubakr O, Metais A, Maillard J, Hasty L, Brigot E, Berthaud C, et al. Utility of combining OLIG2 and SOX10 IHC expression in CNS tumours: promising biomarkers for subtyping paediatric- and adult-type gliomas. *Histopathology.* 2024;84(5): 893–9.

**How to cite this article:** Luo W, Sun C, Jiang Z, Zhang R, Zhang W, Yu S. A 6-year-old female with synchronous cerebellar and thalamic masses. *Brain Pathology.* 2025. e70005. <https://doi.org/10.1111/bpa.70005>